Scripta Materialia 129 (2017) 11–15

Contents lists available at ScienceDirect

Scripta Materialia

journal homepage: www.elsevier.com/locate/scriptamat

Regular article

Shape memory functionality under multi-cycles in NiTiHf

H. Sehitoglu [a,*], Y. Wu [a], L. Patriarca [a,b]

[a] Department of Mechanical Science and Engineering, University of Illinois at Urbana-Champaign Urbana, IL 61801, USA
[b] Politecnico di Milano, Department of Mechanical Engineering, Via La Masa 1, 20156 Milano, Italy

ARTICLE INFO

Article history:
Received 20 May 2016
Received in revised form 23 September 2016
Accepted 9 October 2016
Available online xxxx

Keywords:
Functional fatigue
NiTiHf
Shape memory effect
High temperature shape memory alloy

ABSTRACT

The functionality of NiTiHf (25%Hf) shape memory alloy (SMA) was studied under isobaric temperature cycling experiments. Both the local and overall strains, determined with digital image correlation (DIC), displayed excellent stability and no measurable unrecovered elongation. The external stress levels were higher than 250 MPa and transformation temperature was 420 °C which exceeds other NiTi based alloys, demonstrating the outstanding potential of the NiTiHf alloys.

1. Introduction

The field of shape memory alloys (SMAs) has undergone resurgence in the last decade [1]. The literature has grown dramatically with >5000 papers per year [2] driven by advancements in high temperature, elasto-caloric, ferromagnetic SMAs. New modeling tools [3–5] and high resolution measurements have permitted a deeper understanding of the functional behavior of SMAs from atomic to continuum-levels [6–9]. New alloys have emerged with improved functionalities stimulating further SMA research [10–12]. There is still a need for better understanding of long term functionality, and the origins of degradation in SMAs. Most works to-date have been on the equiatomic NiTi; modifications of this binary system with ternary (such as Hf) and quaternary elements have added unique capabilities [13]. The NiTi based alloys and ternary additions continue to be foundational SMAs for further advancement. In this paper, we focus on the recently discovered NiTiHf (Ti replaced by Hf) alloys that result in unprecedented high temperature shape memory capabilities, large transformation strains and high work outputs [1,7–9,14–16].

At the macro-scales, experiments that characterize the transformation strains, the transformation stresses, and the transformation temperatures have remained the main focus of SMA research. The 'single cycle' (stress or temperature cycle) behavior was investigated in most of the experimental studies [17]. At the same time, the reduction in SMA functionality has been documented under both temperature 'multi-cyles' and superelasticity conditions [18]. In superelasticity experiments, the stress-strain loops do not close and unrecovered strains develop at zero load which accumulate under multi-cycles [18]. In temperature cycling experiments, where the SMA behaves like an actuator, the accumulation of strains at both the high (austenite) and low temperature (martensite) end of the cycle results in ratcheting of strains that exceeds the ductility. A schematic of the trends in SMA response is given in Fig. 1.

During transformation in SMAs, the non-chemical and chemical energy contributions govern the strain-temperature response. Neglecting the non-chemical contribution, the forward (austenite to martensite) and reverse (martensite to austenite) transformations occur at the phase equilibrium temperature, T_o (Fig. 1(a)). In this case, the strain reaches the transformation strain in a stepwise fashion at T_o. The non-chemical free energy consists only of reversible elastic strain energy (Fig. 1(b)). Its presence calls for the need for undercooling below T_o, and in the absence of dissipation, still no hysteresis arises. With dissipative mechanisms such as relaxation of stored elastic strain energy and frictional dissipation at interfaces, further undercooling with respect to T_o is needed. A narrow hysteresis corresponds to minimal energy dissipation ascribed to frictional work and elastic strain energy relaxation while large hysteresis implies high energy dissipation (Fig. 1(c)). Clearly, the irreversible processes on transformation behavior are manifested through the growth of irreversible strain (Fig. 1(d)). The microstructural changes start almost immediately within the first cycle [19] depending on the stress and strain levels and progress with further cycling under constant stress. It is noted that many of the new SMA compositions need to undergo further scrutiny to assess their functionality under 'multi-cycles'.

The functional behavior under fatigue is impacted by two main factors: the occurrence of slip mediated plasticity and the accumulation of residual martensite. Both factors engender deterioration of the shape memory response. The slip mediated plasticity can occur at local scales, particularly at austenite-martensite interfaces where large strain

* Corresponding author.
E-mail address: huseyin@illinois.edu (H. Sehitoglu).

http://dx.doi.org/10.1016/j.scriptamat.2016.10.009
1359-6462/

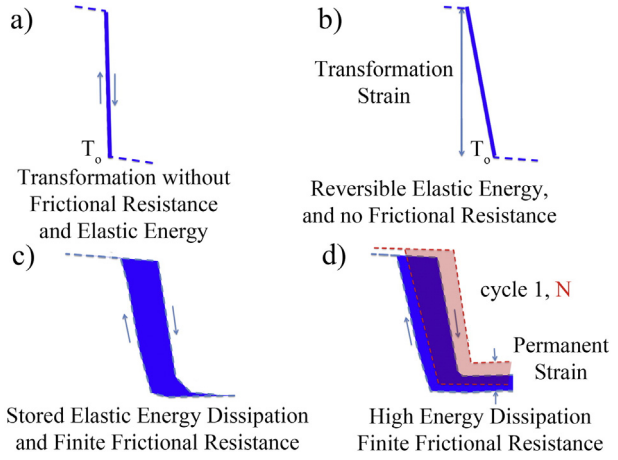

Fig. 1. The schematic strain-temperature response under isostress (tension) temperature cycling experiments on SMA alloys. The transformation strain-temperature in the presence of chemical energy changes without the effects of interface friction and elastic strain energy is shown on case (a). The case in (b) is idealized to show the presence of reversible elastic energy only. The development of permanent strains due to irreversibility upon multi-cycles (Cycle 1, N) is shown in case (d). The growth in the thermal hysteresis (the width of the loop) with multi-cycles is evident. The strain temperature curve (case (c)) shows the case when the SMA response is stable with cycles.

gradients occur. There is continuing debate on the exact steps of the functional deterioration, nevertheless the increase in intrinsic slip resistance is expected to curtail the irreversibility effects and substantially improve SMA functionality. Since the slip resistance of NiTiHf alloys is higher than other SMAs [20], one would anticipate superior functional properties. As an example, the increase in flow stress for the NiTiHf alloys is comparable to the (high Ni) 51.5%Ni NiTi alloys [21]. Remarkably, the transformation strains in NiTi25Hf are near 8%, while the 51.5%Ni NiTi alloys exhibit transformation strains <4%. Moreover, the high temperature SMA capability of NiTiHf is noteworthy. If the functionality is maintained in multi-cycles, the NiTiHf can open new possibilities. In this work, we elaborate on the cyclic performance of NiTiHf alloy with experiments and we also refer to atomistic simulations.

Comprehensive studies on temperature cycling on strain and hysteresis under isobaric conditions have been published in the literature. The compositions in the range 50.1% to 51.5%Ni represent most of nickel contents studied to date. In these early studies, the stress levels have been limited to 150 MPa and the maximum temperature was <100 °C [17]. As stated earlier, the NiTiHf alloys can elevate both stress and transformation temperature levels. The NiTiHf alloys retain the transformation temperatures during cycling as will be demonstrated in our experiments which is beneficial in practical applications.

The presence of precipitates in NiTi alloys is known to modify the SMA behavior [22]. In NiTiHf, the precipitates are orthorhombic, as characterized with diffraction studies [23]. It is believed that the precipitates impart additional slip resistance in these alloys that are beneficial. On the other hand, the precipitates could adversely affect the transformation strains by limiting the detwinning of the internally twinned martensite, hence result in lower transformation strains compared to theory [24].

Previous work on NiTiHf exhibited the shift in transformation temperatures and transformation strains under multi-cycles [15] [25] [26]. These previous careful experiments were conducted under compression and the transformation strains were <4% and 2% in single and polycrystals respectively. Since, based on theoretical considerations the tensile transformation strains are higher, it would be worthwhile to undertake thermal stability and transformation strains experiments exploring the tensile behavior.

To accurately assess the transformation behavior in SMAs, a local measure of the transformation strains is needed as there are elastic (untransforming), partially transformed and transforming domains [7–9,27]. The paper reports on advanced digital image correlation techniques to identify these domains and study their evolution with multi-cycles. Such an insight is very useful compared to bulk measurements (such as with an extensometer) which provide average strain quantities that are not reflective of the progressive evolution at microscale [28].

In summary, in this work, we report on isobaric thermal cycling experiments on NiTi25Hf and investigate the role of cycling on the mechanical response, examining the transformation strains, transformation temperatures and thermal hysteresis. Remarkably, we demonstrate stable transformation temperatures and hysteresis with multi-cycles and enhancements in shape memory strains with cycling. We discuss macroscopic and the local (microscopic) transformation strains levels and illustrate that both follow similar trends with cycling. We also establish the lattice constants for the martensite and provide calculations of the transformation strains discussing the possible reasons for the lower experimental strains compared to the theory. Additionally, we also discuss the need to develop better models to understand functional behavior of SMAs where our understanding is imperfect.

2. Material and experimental procedure

Single crystals of NiTiHf were grown using the Bridgman method and the samples were oriented using high temperature X-ray diffraction. The focus has been on two orientations, the [011] in compression and [111] in tension. The composition of the alloy was measured by means of ICP method as Ni 50.3 at.%, Ti 25% and Hf 24.7%. More details on the crystal orientation measurements and the microstructural data can be found in [27,29].

The tensile and compressive isobaric experiments were conducted by means of an MTS load frame. The temperature was measured by means of a Raytek infrared temperature camera and was manually controlled in order to optimize the DIC image acquisition process. The specimens were cut by electrical discharge machine into 4 mm × 4 mm × 8 mm for the [011] orientation in compression, and into dog bone shape with 3 mm × 1.5 mm gauge section for the [111] orientation in tension. A fine speckle pattern suitable for high resolution DIC strain measurements was deposited on the specimen surface using an Iwata airbrush and a black paint for high temperature applications. The speckle pattern enabled to capture DIC images with a resolution of 3 μm/px. The images for the DIC strain measurements were captured every 5 °C during the isobaric experiments in the 150 °C–450 °C range and successively correlated using a commercial software.

The remarkable attribute of the NiTiHf alloys is that with increasing Hf the monoclinic angle increases, and the theoretical transformation strains increase. Theoretical strain calculations were made using the energy minimization theory to establish the CVP formation strain (twinned martensite) and the lattice deformation theory (single crystal of martensite, detwinned martensite). The results were discussed earlier [22]. The lattice constants for martensite from TEM X ray diffraction results for the NiTi25Hf alloy showed excellent agreement with density functional theory (DFT). The internal twinning in NiTiHf alloys has been identified as Type I and there are compound {001} twins as well.

2.1. Experimental results

The tensile and compressive (isobaric) temperature cycling experiments were conducted and the results are given in Figs. 2 and 3. We note that the experimental results are shown for cycles 1 to 10 in both cases. With the solid lines are represented the strain-temperature curves obtained averaging volume of both transforming and elastic regions (macrostrain). The dashed lines indicate the local strains corresponding to transforming domains. As shown in Fig. 2, in tension, the maximum transformation strain is established as 8.1%. In compression (Fig. 3), the maximum transformation strain is −5.4%. The results are shown for [111] and [011] directions in tension and compression

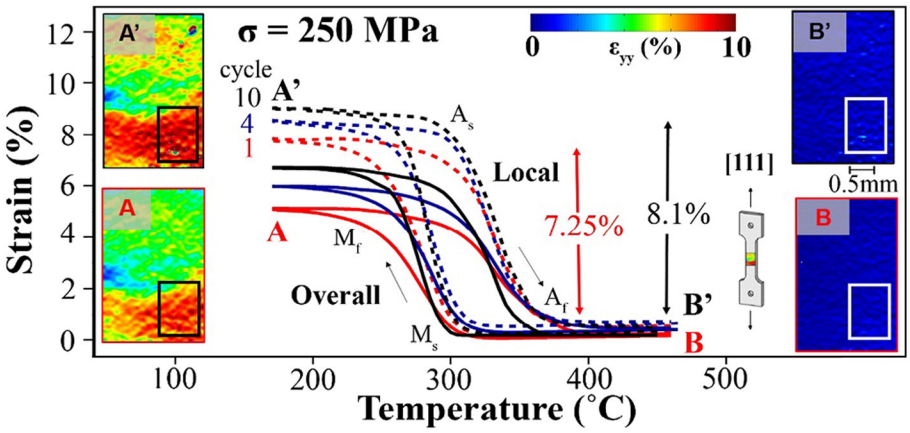

Fig. 2. Strain-temperature results under constant tensile stress in [111] oriented NiTiHf in tension. The local strain was extracted from the rectangular area (1 mm × 2 mm) on the DIC strain contour. Local strain measurements show that the maximum transformation strain increases with cycling from 7.25% to 8.10% after 10 isobaric cycles.

respectively. These orientations are the most favorable ones for tension and compression.

Close examination of results shows that the transformation strains are very stable, and there is no accumulation of permanent strain with cycles. The transformation temperatures, hence the thermal hysteresis, also remain stable under cycling. The austenite finish temperature is near 400 °C while the martensite finish temperature is near 270 °C. This lower temperature shows that the operation temperature of this alloy is in excess of 270 °C. Comparing the local strains (Fig. 2) for the 1st and 10th cycle shows that the transformation domains increased in volume and there is a tendency for the transformation domain to spread to the entire volume.

3. Analysis of results

The theoretical transformation strains for the NiTi25Hf alloy are shown in the Fig. 4a and b using the stereographic triangle. These results are obtained for a monoclinic (B19′) lattice with the lattice constants obtained from DFT analysis (a = 3.09, b = 4.21, c = 4.78, monoclinic angle = 105.9°) and confirmed with selected area diffraction analysis in TEM. There are twelve lattice correspondences between the cubic austenite and monoclinic martensite. We make a distinction between the corresponding variant pair formation (CVP) and the detwinning strain. The CVP corresponds to two martensite variants that are twin related. The detwinning corresponds to the growth one variant with respect to others. In the lattice deformation theory calculations the strains required for transition from single crystal of austenite to single crystal of martensite are calculated. The results of CVP + detwinning strains are very close to LDT calculations. The detwinning strain contribution is significant in tension while it is rather small in compression.

In addition to the transformation strain calculations we conducted DFT simulations of the generalized fault energy and established the unstable and intrinsic fault energies as 516 and 93 mJ/m^2 respectively. These values are utilized in a modified Peierls Nabarro model for calculation of the CRSS for slip in NiTi25Hf. The slip resistance in this alloy is rather high with a value of 614 MPa. In comparison, the other SMAs have much lower values [30].

4. Discussion of results

The mechanical response under isobaric shape memory or superelasticity under multi-cycles must be determined to establish the functional behavior of SMAs. In the present work, we studied the cyclic stability of the isobaric shape memory behavior under temperature cycling. The martensite plate is comprised of correspondent variant pairs, two martensite single crystals (variants) which are twin related. Under isostress conditions, when the temperature is lowered and reaches a critical value, the martensite nucleates and the transformation begins. In the present work, we note that the transformation strains do not reach the detwinned values. With detailed DIC, we note the presence of large elastic domains that do not participate in transformation. This behavior is also observed in the high Ni (51.5%Ni) NiTi alloys [6] where the transformation front does not sweep through the entire specimen and the volume fraction of martensite remains below 1.0. The consequence of such response is that although large strains were measured (>10%) in NiTi25Hf, the theoretical strains (18%) are not attained.

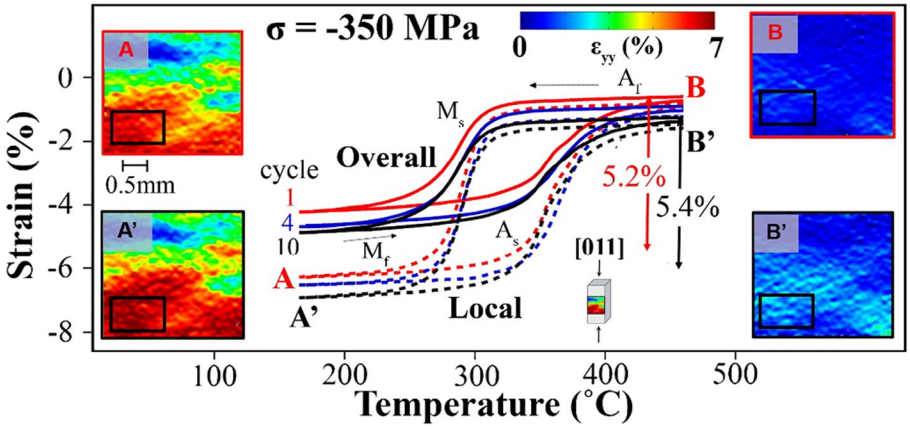

Fig. 3. Strain-temperature results under constant compressive stress in [011] oriented NiTiHf in compression. The local transformation strain reaches 5.4% after 10 isobaric cycles.

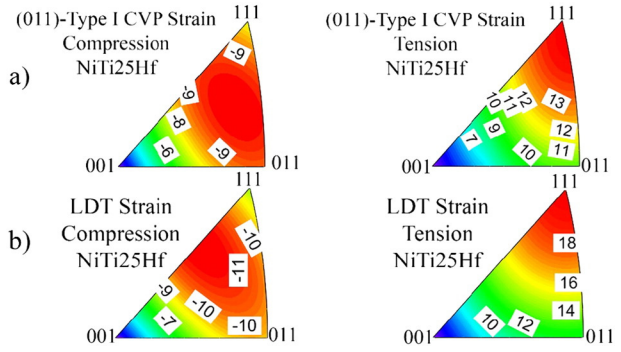

Fig. 4. (a) The CVP formation strain in compression and tension for NiTi25Hf. The CVP formation strains is 9% in compression and 13.4% in tension. (b) The lattice deformation theory strains for single crystal martensite formation in NiTi25Hf. Note the strains at the [111] pole are reaching above 18% in tension.

In NiTi [18,19] and CuZnAl [31] it has been demonstrated that mechanical cycling decreases the magnitude of recoverable transformation strains. The changes occur rapidly often within the first few cycles. Under thermal cycling of NiTiHf, the degradation of shape memory properties has also been observed [32] in past studies. More pronounced degradation under fatigue [33] has been observed at high temperatures. For NiTi8Hf, to improve reversibility severe deformation and grain refinement was considered to increase the slip resistance [26]. In this study, we make the important observation that transformation strains do not degrade with cycling in NiTi25Hf, a highly slip resistant alloy. The transformation temperatures remain stable, and no permanent strain is detected. All these findings point to the favorable characteristics of NiTi25Hf alloys.

Our experiments show that the thermal hysteresis is in the vicinity of 60 °C in tension at 250 MPa while this level increases to 80 °C at 400 MPa in compression. This magnitude of change recognizes that certain level of slip activity must be present; however, we note that a stress level of 400 MPa for thermal cycling is extremely high and exceeds other NiTi alloys. For small increments in stress (such as 50 MPa), the thermal hysteresis change is rather small. Large changes in hysteresis upon cycling are known to be a limiting factor in the utilization of SMAs in applications.

The predicted strains to form a single variant of martensite (LDT strain) were as high as 19% for [111] tension and 9.5% for [011] compression. On the other hand, the predicted CVP formation strains are 13.4% for [111] tension and 9% for [011] compression. Therefore, in compression, the close levels of CVP and LDT strains near the [011] pole and lower experimental strains (5.4%) compared to theory implies minimal detwinning strains. In [111] tension, although the LDT strain is much higher than the CVP strain estimate, the experimental measurement of 8.1% falls far short of the latter, which also implies that the detwinning of martensite may not have occurred. Similar conclusions were drawn in early studies on NiTi [24] and NiTiCu [34] that documented lower experimental strain levels compared to CVP+ detwinning strains predictions. This is an area that requires further study. The slip stress for [011] single crystal in compression is nearly 900 MPa at 450 °C which is remarkably high. This slip stress, which is obtained by conducting compression tests at increasing temperatures, exceeds the transformation stress which is in the range 250 MPa to 600 MPa depending on the temperature. In this study we conducted DFT (Density Functional Theory) calculations using the VASP code. The DFT calculations in this study resulted in a CRSS prediction for slip that is 614 MPa for NiTi25Hf. These calculations utilized the unstable fault energy in conjunction with a modified Peierls-Nabarro model. Using a Schmid factor of 0.5 this would translate to a slip resistance of 1228 MPa for uniaxial stress which is very high. Therefore, the low levels of transformation stress with respect to the very high slip stress creates a favorable condition as the propensity of slip during the transformation is less likely.

The results point to SMA materials that must minimize dissipation due to frictional resistance and elastic strain energy relaxation. If the microstructure consists of austenite-martensite interfaces without the propensity of slip evolution, this will minimize the irreversible processes. The 'idealized' response of NiTi25Hf in this study strongly suggests that irreversible effects in this alloy are curtailed compared to other SMAs.

5. Conclusions

The work supports the following conclusions:

(1) Large transformation strains in NiTi25Hf are possible in comparison to NiTi alloys. The transformation temperatures in NiTi25Hf exceed 400 °C while exhibiting excellent functionality. The high temperature capability could open new applications.
(2) The strain-temperature response of NiTi25Hf under isostress conditions shows remarkable resistance to cyclic degradation under multi-cycles. Considering the occurrence of high strains, such a functionality is unprecedented.
(3) Ultra high slip resistance (CRSS) of 614 MPa was calculated for the monoclinic structure combining the fault energetics with a modified Peierls–Nabarro calculation procedure. The transformation stresses are well below the theoretical CRSS value ensuring recoverability under multi-cycles.

Acknowledgements

The work was supported by NSF CMMI–1333884. This support is gratefully acknowledged. We acknowledge Prof. Chumlyakov for growing the single crystals. Mr. Avinesh Ojha calculated the slip stress for NiTi25Hf monoclinic lattice.

References

[1] J. Ma, I. Karaman, R.D. Noebe, Int. Mater. Rev. 55 (2010) 257–315.
[2] H. Sehitoglu, Shap. Mem. Superelasticity 1 (2015) 1–3.
[3] T. Ezaz, J. Wang, H. Sehitoglu, H.J. Maier, Acta Mater. 61 (2013) 67–78.
[4] M.F.X. Wagner, W. Windl, Acta Mater. 56 (2008) 6232.
[5] N. Hatcher, O.Y. Kontsevoi, A.J. Freeman, Physical Review B (Condensed Matter and Materials Physics) 80 (2009), 144203 (18 pp.).
[6] C. Efstathiou, H. Sehitoglu, Scr. Mater. 59 (2008) 1263–1266.
[7] L. Patriarca, Y. Wu, H. Sehitoglu, Y.I. Chumlyakov, Scr. Mater. 115 (2016) 133–136.
[8] Y. Wu, L. Patriarca, G. Li, H. Sehitoglu, Y. Soejima, T. Ito, et al., Shap. Mem. Superelasticity 1 (2015) 387–397.
[9] Y. Wu, L. Patriarca, H. Sehitoglu, Y. Chumlyakov, Scr. Mater. 118 (2016) 51–54.
[10] Y. Tanaka, Y. Himuro, R. Kainuma, Y. Sutou, T. Omori, K. Ishida, Science 327 (2010) 1488–1490.
[11] Y. Sutou, N. Kamiya, T. Omori, R. Kainuma, K. Ishida, K. Oikawa, Appl. Phys. Lett. 84 (2004) 1275.
[12] J.I. Kim, H.Y. Kim, H. Hosoda, S. Miyazaki, Mater. Trans. 46 (2005) 852–857.
[13] K. Otsuka, X. Ren, Prog. Mater. Sci. 50 (2005) 511.
[14] A.P. Stebner, G.S. Bigelow, Y. Jin, D.P. Shukla, S.M. Saghaian, R. Rogers, et al., Acta Mater. 76 (2014) 40–53.
[15] H.E. Karaca, S.M. Saghaian, G. Ded, H. Tobe, B. Basaran, H.J. Maier, et al., Acta Mater. 61 (2013) 7422–7431.
[16] R. Santamarta, R. Arróyave, J. Pons, A. Evirgen, I. Karaman, H. Karaca, et al., Acta Mater. 61 (2013) 6191–6206.
[17] R.F. Hamilton, H. Sehitoglu, Y. Chumlyakov, H.J. Maier, Acta Mater. 52 (2004) 3383.
[18] S. Miyazaki, T. Imai, Y. Igo, K. Otsuka, Metallurgical Transactions A (Physical Metallurgy and Materials Science) 17A (1986) 115–120.
[19] K. Gall, H. Sehitoglu, Y.I. Chumlyakov, L.V. Kireeva, Scr. Mater. 40 (1998) 7.
[20] J. Wang, H. Sehitoglu, Philos. Mag. 94 (2014) 2297–2317.
[21] H. Sehitoglu, J. Jun, X. Zhang, I. Karaman, Y. Chumlyakov, H.J. Maier, et al., Acta Mater. 49 (2001) 3609–3620.
[22] H. Sehitoglu, I. Karaman, R. Anderson, X. Zhang, K. Gall, H. Maier, et al., Acta Mater. 48 (2000) 3311–3326.
[23] D.L. Medlin, C.B. Carter, J.E. Angelo, M.J. Mills, Philosophical Magazine A 75 (1997) 733–747.
[24] H. Sehitoglu, R. Hamilton, D. Canadinc, X.Y. Zhang, K. Gall, I. Karaman, et al., Metallurgical and Materials Transactions A: Physical Metallurgy and Materials Science 34 (2003) 5.
[25] S. Besseghini, E. Villa, A. Tuissi, Mater. Sci. Eng. A 273–275 (1999) 390–394.
[26] B. Kockar, I. Karaman, J.I. Kim, Y. Chumlyakov, Scr. Mater. 54 (2006) 2203–2208.

[27] Patriarca L, Sehitoglu H. High-temperature superelasticity of Ni50.6Ti24.4Hf25.0 shape memory alloy. Scr. Mater.
[28] C. Efstathiou, H. Sehitoglu, J. Carroll, J. Lambros, H.J. Maier, Acta Mater. 56 (2008) 3791–3799.
[29] L. Patriarca, HS, Y. Chumlyakov, Acta Mater. (2016) (to appear).
[30] J. Wang, H. Sehitoglu, H.J. Maier, Int. J. Plast. (2013) (In press).
[31] M. Sade, E. Hornbogen, Zeitschrift fur Metallkunde 79 (1988) 782–787.
[32] X.L. Meng, Y.F. Zheng, Z. Wang, L.C. Zhao, Mater. Lett. 45 (2000) 128–132.
[33] O. Matsumoto, S. Miyazaki, K. Otsuka, H. Tamura, Acta Metall. 35 (1987) 2137–2144.
[34] H. Sehitoglu, I. Karaman, X. Zhang, H. Kim, Y. Chumlyakov, I. Kireeva, et al., Metall. Mater. Trans. A 32 (2001) 477–489.